International Journal of Precision Engineering and Manufacturing-Green Technology (2020) 7:929–938
https://doi.org/10.1007/s40684-019-00176-4

Online ISSN 2198-0810
Print ISSN 2288-6206

REGULAR PAPER

Removal of Contaminant Nanoparticles with CO_2 Nanobullets at Atmospheric Conditions

Jae Hong Lee[1] · Joonoh Kim[1] · Seungho Kim[1] · Joongha Lee[1] · Jinkyu Kim[2] · Kihoon Choi[2] · Ho-Young Kim[1,3]

Received: 6 August 2019 / Revised: 23 October 2019 / Accepted: 21 November 2019 / Published online: 17 December 2019

Abstract
As the feature size of semiconductor chips is decreasing down to nanometric scales, cleaning of nanoscale contaminant particles without damaging the fine features puts forth severe technological challenges. Here we introduce a design methodology of a nozzle to generate a beam of supersonic CO_2 solid nanobullets into the air at atmospheric pressure, which dislodge the contaminant particles by colliding with them. The dry cleaning scheme proposed here does not resort to the chillers, vacuum chamber, and carrier-gas handling system, which conventional dry cleaning systems often required and thus hampered their practical applications. We provide a theoretical framework to select key design parameters, such as the area ratio of the nozzle throat and exit and the supply gas pressure. We experimentally verify the superior capability of our nozzle in generating a CO_2 aerosol beam under the atmospheric back pressure condition. Additional process parameters including the stand-off distance and the incident angle of the CO_2 beam are optimized to maximize the cleaning efficiency and minimize the pattern damages. Our work suggests a practical nanoparticle cleaning scheme that is faster and simpler than the conventional dry cleaning methods.

Keywords Compressible flow · Supersonic nozzle · Sublimation · Nanoparticle removal

1 Introduction

Cleaning of wafers and photomasks constitutes important processes in semiconductor manufacturing as it plays a critical role in determining the yield and quality of the products [1]. With the continual decrease of feature sizes in semiconductor devices below tens of nanometers, the size of killer particles having a fatal effect on the circuit performance is also decreasing [2]. The finer the contaminant particles, the stronger the adhesion force gets per contact area of the particle and the substrate. Therefore, effective techniques to dislodge nanometric contaminant particles without damaging fine and fragile functional components are strongly desired.

The cleaning methods of semiconductors are classified into wet and dry schemes. In the wet cleaning, one often uses liquid chemicals (e.g., hydrogen peroxide, ammonium hydroxide, hydrofluoride, etc) or ultrasonic waves to dislodge contaminants through etching, electrostatic repulsion or hydrodynamic forcings [3–7]. Despite their strong cleaning ability, the wet schemes may generate environmentally harmful wastes [8], leave residual precipitates after drying [9], and lead to collapse or leaning of submicrometric patterns by capillary forces of drying liquid films [10–12]. The dry schemes use jets of fine solid particles of argon, nitrogen or carbon dioxide, which collide with contaminants and transfer momentum to disengage them from the substrate. They are in general environmentally benign and free of those problems associated with evaporation of liquid chemicals. The cryogenic aerosol techniques generate particle-laden jets by drastic expansion of cryogenic fluid (argon or nitrogen) which is pre-cooled to below 100 K [13, 14]. CO_2 needs no cryogenic cooling because its sublimation temperature is much higher (194.7 K) than that of Ar (83.8 K) or N_2

Jae Hong Lee and Joonoh Kim have contributed equally to this work.

✉ Ho-Young Kim
hyk@snu.ac.kr

[1] Department of Mechanical and Aerospace Engineering, Seoul National University, Seoul 08826, Korea

[2] R&D Center, SEMES Co., Ltd., Hwaseong-si, Gyeonggi-do 18383, Korea

[3] Institute of Engineering Research, Seoul National University, Seoul 08826, Korea

(63.1 K). Because the CO_2 gas used for the cleaning process is captured from the natural environment, no additional environmental contamination is generated, which prompted replacement of some hazardous chemicals with CO_2 in other manufacturing industries[15, 16].

Removal of contaminant particles tens of nanometers in size using CO_2 nanoparticle jets were reported earlier [17–19]. Despite previous demonstrations of the CO_2-based cleaning method, the following aspects should be further improved for the scheme to be employed in the actual fabrication line. First, all the previous researches needed to control the temperature and pressure of the cleaning chamber to achieve sufficient momentum of CO_2 particles. In particular, the cleaning chamber was at vacuum conditions, which lowered the fabrication rate while increasing the cost and energy consumption. Second, an additional carrier gas like helium was frequently used to accelerate the particles. Third, the operation conditions to avoid damages of functional patterns while maintaining a high cleaning efficiency were seldom established. Therefore, here we report an apparatus capable of issuing CO_2 nanoparticles with a sufficient momentum for cleaning in a chamber at atmospheric pressure and room temperature. We also provide the conditions to achieve high cleaning efficiency without damaging nanopatterns. This apparatus provides huge advantages to reduce cost and complexity of the actual fabrication scene in that no additional facilities are necessary like chillers, vacuum pumps, and He injection systems.

In the following, we start with a description of the cleaning system, and explain the theoretical approaches to obtain the nozzle design to issue CO_2 nanoparticles with a high velocity into the air at atmospheric pressure. Then we provide the results to visualize the nanobullet jets, or CO_2 beam, to measure the removal efficiency of contaminant particles, and to evaluate the pattern damages, under varying experimental conditions. Our experiments allow us to find the optimal operation conditions for a high cleaning efficiency and minimal pattern damages.

2 Experimental

The experimental apparatus to generate high-speed CO_2 beams is schematically depicted in Fig. 1a. The compressed CO_2 gas is supplied to a plenum chamber, whose large volume effectively stops the CO_2 gas and regulates the pressure and temperature. The pressure loss from the gas tank to the plenum chamber is negligible while the temperature in the plenum chamber is kept at 298 K. Then the high-pressure gas enters a nozzle where the gas passage converges and

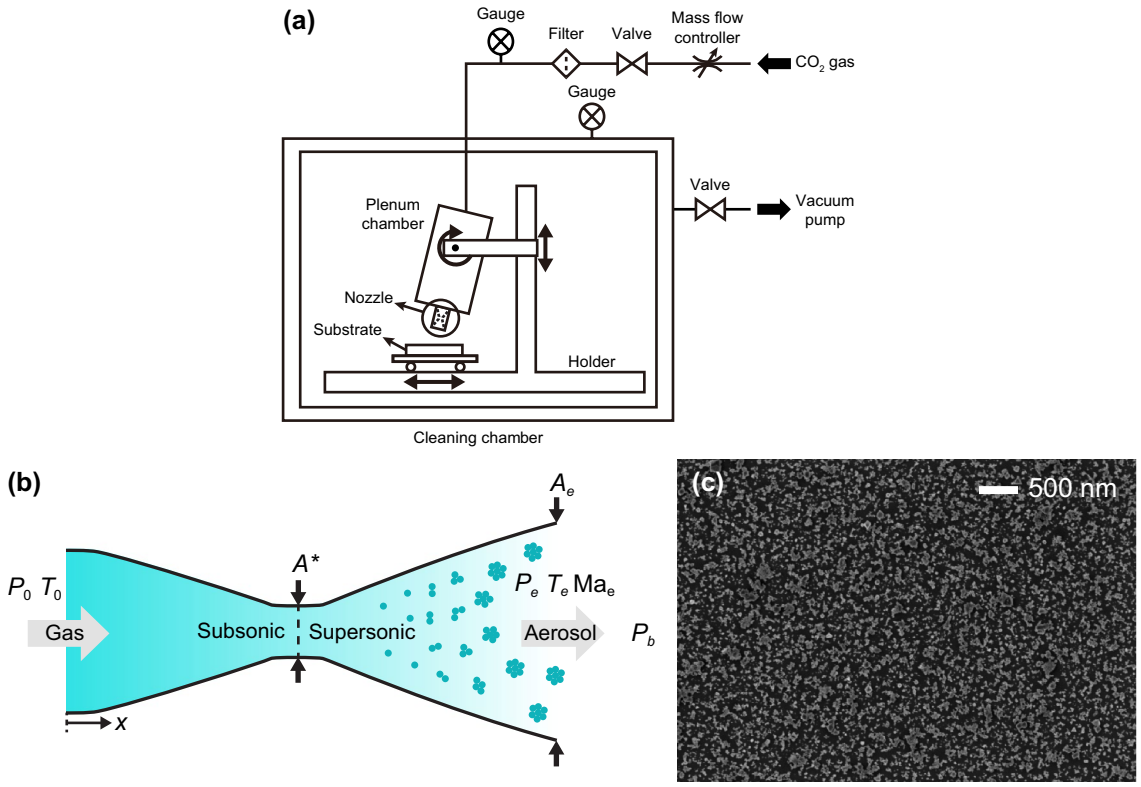

Fig. 1 **a** Schematic of the experimental apparatus for CO_2 beam cleaning. **b** The generation process of an CO_2 aerosol beam with a converging-diverging nozzle, which is enclosed by a circle in **a**. **c** SEM image of the silicon wafer contaminated with the sub-25-nm particles of CeO_2

then diverges as shown in Fig. 1b. As will be explained in detail below, the gas is accelerated in the converging section. Upon passing the neck, the gas undergoes sudden expansion accompanying a drastic decrease in pressure and temperature. Then the supersonic CO_2 gas sublimates into solid particles, which grow in size to reach several tens of nanometers. The velocity and size of the issued CO_2 particles depend on the pressure and temperature at both ends of the nozzle and the nozzle geometry.

The CO_2 particles are injected into the cleaning chamber and directly collide with contaminant particles on a wafer. The interior pressure of the cleaning chamber ranges from 0.05 to 1 bar as controlled by a vacuum pump, while its temperature is kept at 298 K. The distance from the nozzle exit to the wafer surface, and the incident angle of the CO_2 beam can be adjusted. The wafer moves horizontally at 3 mm/s to ensure cleaning of wide surface area. We visualize the CO_2 beams issued from the nozzle with a high-speed camera (Fastcam SA-Z, Photron).

We evaluate the cleaning efficiency by analyzing the images of a contaminated wafer before and after cleaning with the scanning electron microscope (SEM). To contaminate the wafer surface, we uniformly spin-coat the wafer with spherical nanoparticles of CeO_2 (Sigma Aldrich), whose diameter ranges from 4 to 13 nm, as shown in Fig. 1c. The particle removal efficiency, η, is defined as $\eta = (A_b - A_a)/A_b$, where A_b and A_a is the surface area covered by the contaminants before and after cleaning, respectively. We identify the covered area by binarizing grey value of each pixel in the SEM images based on the threshold brightness. We evaluate η on the area of 0.06 mm^2 of the wafer surface and average them.

3 Aerothermal Design of Nozzle

To generate supersonic CO_2 solid nanobullets, we use a conical, converging-diverging nozzle as shown in Fig. 1b. While previous researches used converging-diverging nozzles to issue CO_2 beams in a vacuum chamber [17–19], here we introduce a design methodology and associated theoretical developments to determine the nozzle dimensions that enable strong and stable jets of CO_2 solid nanoparticles into an atmospheric condition. The gas flow entering the nozzle undergoes phase change in the diverging section, which can cause great complexity in theoretical analysis and nozzle design. We employ a single-phase compressible flow theory throughout the nozzle for a low mass fraction of solid in the CO_2 stream [20, 21]. In the following, we explain how to determine the key design parameter of the nozzle, i.e. the ratio of the cross-sectional areas of exit and throat, and the gas supply pressure, both of which depend on the target Mach number at the exit.

We start with the range of the Mach number at the exit which ensures the stable jet in the atmospheric pressure condition. When the pressure of the exiting gas differs from the back pressure (the pressure in the cleaning chamber), the CO_2 beam experiences abrupt pressure change, leading to shocks [22–24]. Then the velocity, density, pressure and temperature of the issued CO_2 beam fluctuate [25], and the CO_2 particles cannot maintain sufficient momentum to dislodge contaminant particles. Hence, the exit pressure P_e should match the atmospheric pressure.

The CO_2 at the nozzle inlet needs to be supplied as gas phase rather than a supercritical fluid. When the aerosols are generated from the critical state, the particles experience prolonged condensation and growth in the nozzle, resulting in undesired size increase [19]. Excessively large particles are ineffective in removing finer contaminant particles while only increasing the possibility of pattern damages. Thus, the stagnation pressure P_0 (the pressure at the nozzle inlet or in the plenum chamber) should be lower than the liquefaction pressure of CO_2 at 298 K, 64.3 bar [26]. The aerodynamic theory states that the Mach number at the exit of the converging-diverging nozzle, $\mathrm{Ma}_e = U_e/a$ with U_e and a respectively being the exit flow velocity and speed of sound at 298 K, is related to the pressure ratio P_0/P_e as [27]

$$\frac{P_0}{P_e} = \left(1 + \frac{k-1}{2}\mathrm{Ma}_e^2\right)^{k/(k-1)}, \tag{1}$$

where $k = 1.3$ is the specific heat ratio of CO_2 gas and an adiabatic process is assumed. Here we assume P_0 to be high enough to ensure that the Mach number at the nozzle throat is unity. Because $P_e = 1$ bar and $P_0 < 64.3$ bar, Ma_e should be less than 3.27.

The lower bound of Ma_e is given by the temperature consideration. Through the diverging section, the temperature of the gas drops due to the adiabatic expansion. To generate solid phase CO_2 clusters before escaping the nozzle, the temperature of CO_2 at the nozzle exit, T_e, should be lower than the sublimation temperature, 194.5 K for atmospheric pressure. Ma_e and T_e are interrelated as [27]

$$\frac{T_0}{T_e} = 1 + \frac{k-1}{2}\mathrm{Ma}_e^2, \tag{2}$$

where T_0 is the stagnation or inlet temperature, 298 K. For $T_e < 194.5$ K, Ma_e should be higher than 1.84.

Within the range of the target Mach number, $1.84 < \mathrm{Ma}_e < 3.27$, that satisfies the foregoing pressure and temperature conditions, a high Ma_e is preferred to transfer sufficient momentum to the contaminants. We set $\mathrm{Ma}_e = 3.17$ in our design to avoid likely liquefaction and excessive fluid consumption when Ma_e is too close to the upper bound, 3.27. This value allows us to determine the

ratio of the nozzle exit area (A_e) to the throat area (A_t) to be 6.25 using the following relationship [27]:

$$\frac{A_e}{A_t} = \frac{1}{\mathrm{Ma}_e}\left[\frac{2+(k-1)\mathrm{Ma}_e^2}{k+1}\right]^{\frac{1}{2}(k+1)/(k-1)}. \tag{3}$$

We also find $P_0 = 50$ bar and $T_e = 119$ K to yield $\mathrm{Ma}_e = 3.17$ using Eqs. (1) and (2), respectively.

To verify the foregoing theoretical development based on the single-phase flow assumption, we now obtain the pressure, temperature and Mach number of CO_2 gas considering the phase change. Hill [28] developed a one-dimensional model that predicts the states of the gas flowing through a supersonic nozzle including the phase transition as follows:

$$\frac{\mathrm{d}P}{\mathrm{d}x} = \frac{P\left[(\lambda-1)\frac{\mathrm{d}\mu}{\mathrm{d}x} - \frac{1}{A}\frac{\mathrm{d}A}{\mathrm{d}x}\right]}{1-(1-\mu)\left(\frac{k-1}{k}+\frac{1}{k\mathrm{Ma}^2}\right)}, \tag{4}$$

$$\frac{\mathrm{d}T}{\mathrm{d}x} = T\left[\lambda\frac{\mathrm{d}\mu}{\mathrm{d}x} + \frac{k-1}{k}(1-\mu)\frac{1}{P}\frac{\mathrm{d}P}{\mathrm{d}x}\right], \tag{5}$$

$$\frac{\mathrm{dMa}}{\mathrm{d}x} = -\mathrm{Ma}\left[\frac{(1-\mu)\frac{1}{P}\frac{\mathrm{d}P}{\mathrm{d}x}}{k\mathrm{Ma}^2} + \frac{1}{2T}\frac{\mathrm{d}T}{\mathrm{d}x}\right], \tag{6}$$

where $\lambda = h_{fg}/(c_pT)$ with h_{fg} and c_p respectively being the enthalpy change during the phase transition and the specific heat at constant pressure, x is the distance from the entrance of the nozzle, μ is the mass ratio of solid to vapor, and A is the cross-sectional area of the nozzle at x. The theory predicts the path of P and T of the gas in the nozzle, starting from the supply condition of 50 bar and 298 K and reaching 0.93 bar and 118 K at the exit, as depicted in Fig. 2. These values are fairly close to the foregoing results(1 bar and 119 K) that ignored the phase change. Because the CO_2 gas passes through the nozzle in a few microseconds, the time for heat transfer during the phase change is too short for the sublimation to exert significant effects on P and T of the gas.

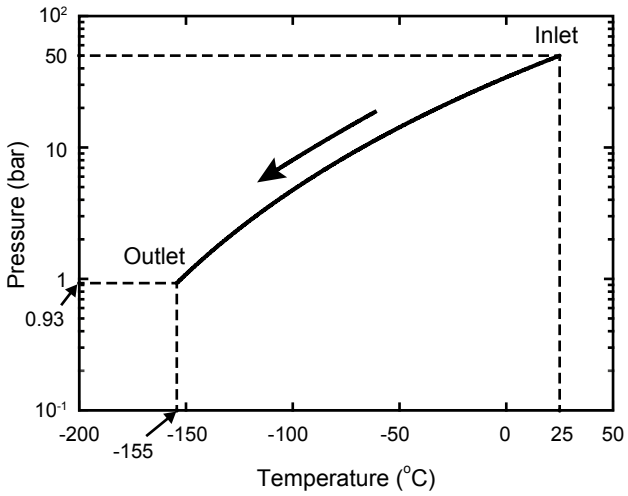

Fig. 2 Theoretical path of the pressure and temperature of the CO_2 flowing through the supersonic nozzle with $A_e/A_t = 6.25$, obtained by using Eqs. (4–6)

4 Results and Discussions

4.1 Visualization of Supersonic CO_2 Beam

We experimentally observe the shape of CO_2 aerosol beam generated from the nozzle designed as above while changing the back pressure P_b, i.e. the pressure in the cleaning chamber, from 0.05 to 1 bar. CO_2 gas is supplied to the plenum chamber at 50 bar and 298 K. The images of CO_2 beam under different back pressure are shown in Fig. 3. The Rayleigh scattering of light off the CO_2 nanoparticles allow us to visualize the CO_2 beam in blue. We see that as the back pressure increases, the CO_2 beam becomes thinner without diverging near the nozzle exit and clearer in color. For the lower pressure, Fig. 3a–d, the ejected CO_2 beam undergoes abrupt pressure changes forming an underexpanded jet [22] because the gas pressure at the nozzle exit is designed to match the atmospheric pressure. The issued CO_2 gas forms expansion waves accompanying fluctuations in temperature, pressure, and density. Thus, the solid CO_2 particles generated in the nozzle are prone to re-sublimation, resulting in a dim beam in Fig. 3a. Figure 3c shows bumpy outlines of the jet and Mach disks [23, 25], characteristics of the expansion waves. Under the atmospheric back pressure condition, Fig. 3f, the diameter of the beam changes little as traveling downstream, enabling the CO_2 particles to stay as solid and to carry sufficient momentum until collision with contaminants.

To see the effects of nozzle design on the formation of a CO_2 beam, we observe the beam issued from a nozzle specialized for vacuum back pressure [17–19]. The area ratio A_e/A_t of the nozzle is 289, which achieves the exit Mach number of 7 [17, 27]. The pressure and temperature of the supplied gas at the plenum chamber are 50 bar and 298 K. Figure 4 shows that the CO_2 beam, which is clearly visible at the back pressure of 0.05 bar in (a), tends to vanish as the back pressure increases. Because the pressure of the exiting CO_2 is tuned to be low, the CO_2 aerosol is compressed and decelerated under high back pressure. The normal shocks are generated in the nozzle due to large pressure difference across the nozzle exit [23, 24, 29]. The CO_2 particles are re-sublimated in the nozzle, failing to form a stable beam.

Upon verifying the effectiveness of our nozzle design in issuing a clear beam of CO_2 under atmospheric back

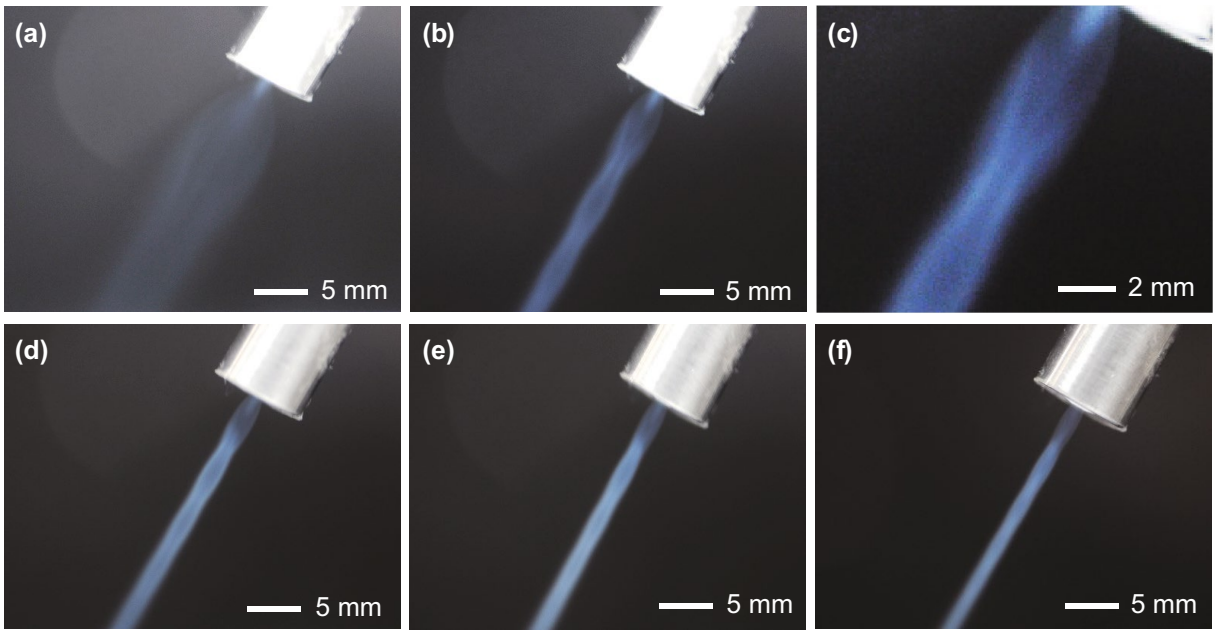

Fig. 3 The shape of CO_2 beam issued from the nozzle with $A_e/A_t = 6.25$ under various cleaning chamber pressure. **a** $P_b = 0.05$ bar. **b** $P_b = 0.25$ bar. **c** An enlarged image of the CO_2 beam of **b**. **d** $P_b = 0.5$ bar. **e** $P_b = 0.75$ bar. (f) $P_b = 1$ bar

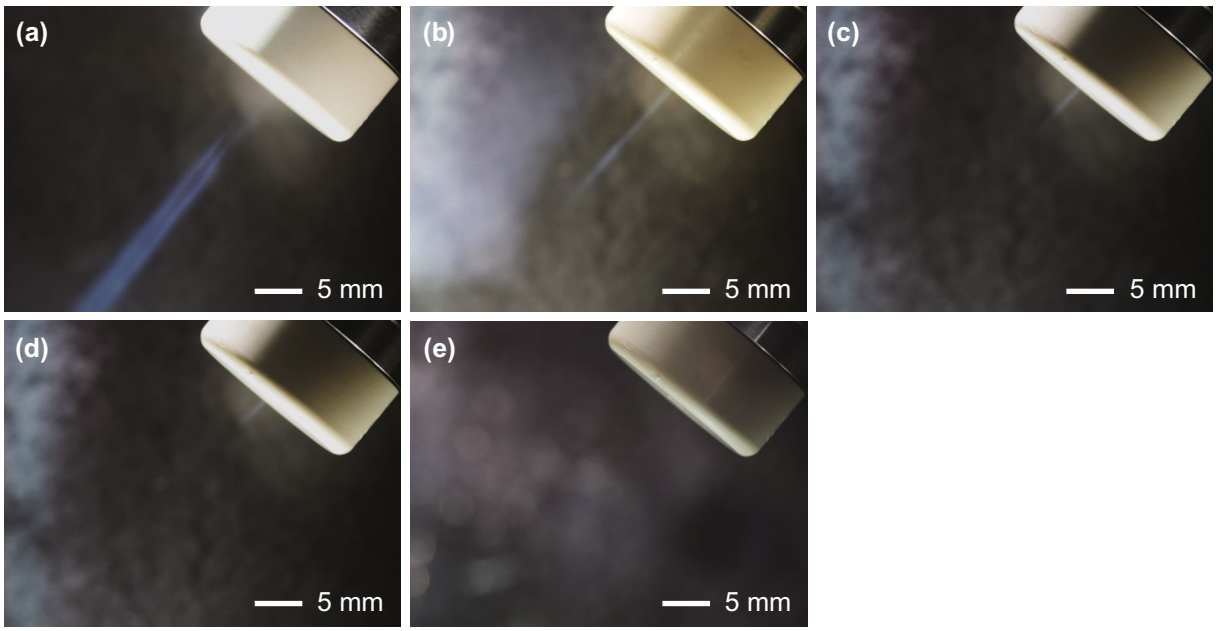

Fig. 4 The shape of CO_2 beam issued from the nozzle with $A_e/A_t = 289$ under various cleaning chamber pressure(back pressure). **a** $P_b = 0.05$ bar. **b** $P_b = 0.25$ bar. **c** $P_b = 0.5$ bar. **d** $P_b = 0.75$ bar. **e** $P_b = 1$ bar

pressure, we now turn to examine the states of CO_2 in the beam of Fig. 3f. By collecting the CO_2 beam impacting on a Si wafer 1 cm away from the nozzle, we find a white hill to form as shown in Fig. 5a, resulting from the accumulation of solid particles of CO_2. We also issue the CO_2 particles onto a substate coated with 2 μm-thick photoresist (AZ 5214E) under atmospheric condition, to find dents caused by solid impacts as shown in Fig. 5b. The average width of the dents is 36 nm with the standard deviation of 15 nm, giving us the size of CO_2 nanobullets.

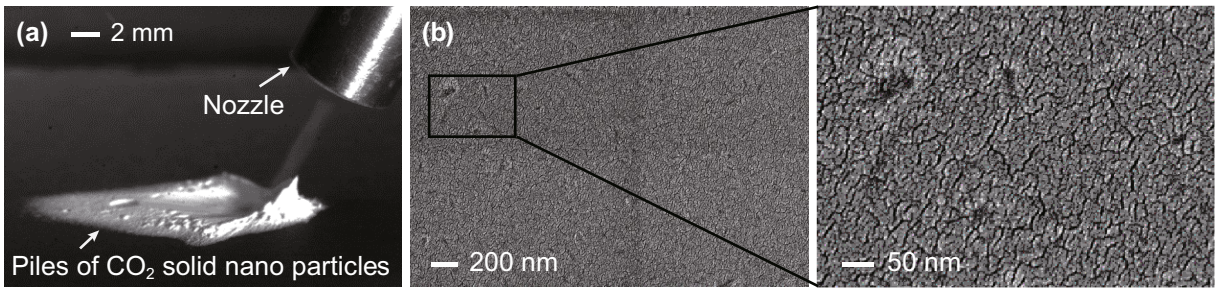

Fig. 5 **a** Piles of solid CO_2 particles. **b** SEM images of a photoresist film bombarded by CO_2 beam. The distance from the nozzle tip to the substrate is 3 cm, and the incident angle is 90°

4.2 Effects of Stand-Off Distance and Incident Angle

With the supersonic CO_2 particles issued from the nozzle, we now evaluate the effects of the stand-off distance and incident angle of the beam on the cleaning efficiency. We vary the incident angle α, the angle between the beam and the flat substrate, from 30° to 90°. The stand-off distance, l, measured from the nozzle exit to the substrate in the direction parallel to the beam, ranges from 2 to 4 cm. Figure 6a shows the experimentally measured particle removal efficiency at different l and α.

Regardless of the incident angles, η is maximized when l ranges from 3 to 3.5 cm. When $\alpha = 45°$, η at $l = 3$ cm is approximately 6% and 23% higher than those at $l = 2$ and 4 cm, respectively. We attribute this dependency of η on l to the size and speed of the impacting particles. The solid CO_2 particles issued from the nozzle decrease in size during flight for heat exchange with the atmosphere. The Mach number of the issued particles also decreases due to the air drag. For $l < 3$ cm, the CO_2 particles are supposed to arrive at the substrate with excessively large size, which was reported to be inefficient in removing sub-micrometric particles [30]. When the stand-off distance is too large, $l > 3.5$ cm, the velocity of the CO_2 particles is too small to transfer sufficient momentum to the contaminants.

We see in Fig. 6a that at the same stand-off distance, the higher η is obtained in general as the incident angle decreases. When $l = 3$ cm, η at $\alpha = 30°$ is 7% higher than at $\alpha = 90°$. It is because the particulate contaminants, which are non-spherical due to attractive interactions with the substrate [31], are dislodged dominantly by the sliding mechanism [30, 32] upon collision with CO_2 nanobullets. As the horizontal impact force of the nanobullets increases with reduced α, it is more likely that the static friction force of the contaminant particles is overcome, which is proportional to the vertical component of the impact force.

It is known that the minimum speed of CO_2 bullets required to remove contaminant particles decreases as the contaminants get larger [30]. Hence, our experiments using contaminant particles with the diameter ranging from 4 to 13 nm allow us to examine whether our process conditions are sufficient to remove particles over 10 nm in diameter. The

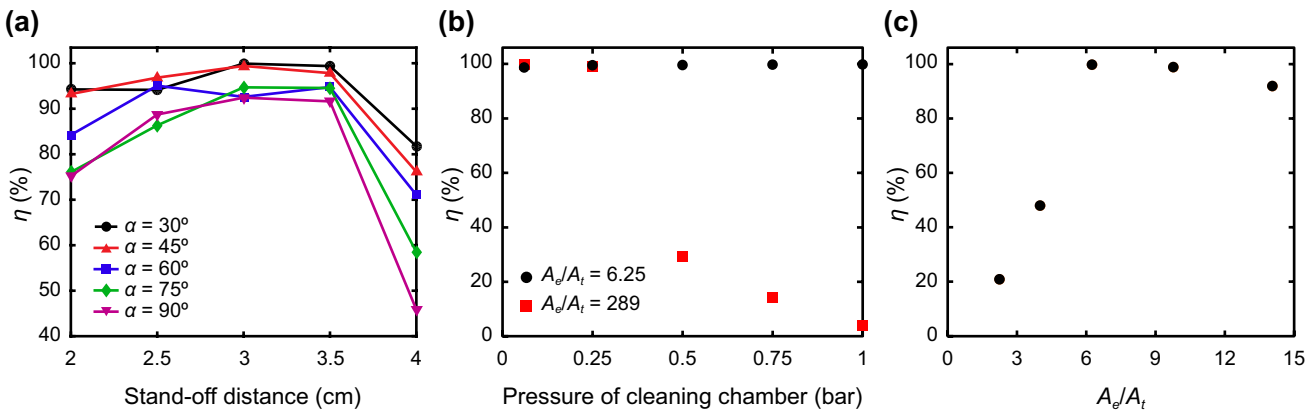

Fig. 6 **a** Particle removal efficiency for varying stand-off distance and incident angle using a nozzle with $A_e/A_t = 6.25$. **b** Particle removal efficiency versus pressure of the cleaning chamber. Black circles and red squares correspond to $A_e/A_t = 6.25$ and 289, respectively. **c** Particle removal efficiency versus the area ratio A_e/A_t. The data points are the averages of 4 measurements for each cleaning condition, and the error bars are smaller than the size of symbols

cleaning of the contaminants of the order of 1 nm in size would require further experiments with finer contaminant particles.

Impacts of CO_2 nanobullets can damage submicrometric patterns. To see the effects of the particle impact conditions on the pattern damages, we clean an array of line patterns contaminated with the sub-25-nm size CeO_2 particles as shown in Fig. 7a. The line patterns of SiO_2 have the width, height, and yield strength of 500 nm, 2.6 µm, and 55 MPa, respectively. At a distance where the cleaning of flat substrates is the most efficient, $l = 3$ cm, we use the incident angles 10° and 45°. The CO_2 beam scans the substrate in a direction perpendicular to the longitudinal direction of the line patterns at the speed of 3 mm/s. When $\alpha = 45°$, Fig 7b, no pattern damage is observed with the particle removal efficiency reaching 99%. But for $\alpha = 10°$, Fig 7c, we see damaged patterns despite almost perfect removal of contaminant particles. These results suggest that while the increased horizontal component of particle impact force with low α is beneficial for cleaning, excessively low α should be avoided to prevent pattern damage. For the current cleaning system, the stand-off distance of 3 cm and the incident angle of 45° lead to the most desirable cleaning performance with no pattern damages.

4.3 Effects of Back Pressure and Nozzle Design

We evaluate the cleaning efficiency of the supersonic CO_2 beam issued from the nozzle designed for the atmospheric condition under different back pressure, or the pressure in the cleaning chamber. The experimental results of the particle removal efficiency with $l = 3$ cm and $\alpha = 45°$ are displayed in Fig. 6b. We see that the particle removal efficiency decreases but slightly as the back pressure decreases, from 99.8% at 1 bar to 98.6% at 0.05 bar. As shown in Fig. 3, the abrupt pressure changes from the design value, 1 bar, to the lower back pressure give rise to expansion waves. At the same time, however, the ejected CO_2 can be further accelerated even outside the diverging nozzle when $P_b < 1$ bar. Despite the fluctuations of the properties of the CO_2 caused by the expansion waves, this acceleration is supposed to help the beam to maintain the strong cleaning ability.

In addition to the nozzle designed for the atmospheric pressure, we evaluate the cleaning efficiency of the aforementioned nozzle designed for the vacuum with $A_e/A_t = 289$ under different back pressure. Figure 6b shows that the particle removal efficiency decreases drastically as the back pressure increases from 0.05 bar to 1 bar. As shown in Fig. 4, the CO_2 from this nozzle is compressed and decelerated under normal shock waves while the CO_2 particles are re-sublimated to gas for $P_b > 0.05$ bar. The poor particle removal efficiency at high P_b is consistent with the vanishing CO_2 beams in Fig. 4b–e.

To further check the effects of the area expansion ratio, A_e/A_t, on the particle removal efficiency, we measure η while changing the ratio from 2.25 to 14.06 and plot the results in Fig. 6c. The back pressure, stand-off distance, and incident angle are 1 bar, 3 cm, and 45°, respectively. As the area ratio decreases from 6.25 to 2.25, η decreases steeply. For the area ratios lower than 6.25, the exit pressure becomes higher than 1 bar, as given by Eq. (1), which leads to expansion waves while traveling in the cleaning chamber. Furthermore, the Mach number at the nozzle exit decreases according to Eq. (3), implying the decreased momentum of the impacting CO_2 particles, which is considered a major cause of the reduced particle removal efficiency. For the area ratios higher than 6.25, η decreases rather gradually, which will be eventually very low as already shown for $A_e/A_t = 289$ in Fig. 6b. When the area ratio is higher than 6.25, the pressure at the nozzle exit is lower than the atmospheric pressure, Eq. (1), inducing shock waves. But the Mach number increases as the area ratio increases, Eq. (3), implying enhanced momentum of impacting CO_2 particles. Thanks to this high velocity of the CO_2 beam, the particle removal efficiency does not reduce as steeply as the case for the lower area ratios.

Fig. 7 SEM images of the line-patterned SiO_2 wafer before and after cleaning. **a** The line-patterned surface contaminated with CeO_2 particles before cleaning. Black lines are the gap between the line patterns and white dots are the CeO_2 particles. **b** The patterned surface cleaned with the incident angle of $\alpha = 45°$. **c** The patterned surface cleaned with the incident angle of $\alpha = 10°$

5 Conclusions

As a viable solution to the problems associated with removing contaminant nanoparticles using wet chemicals, we presented a methodology to design a nozzle that issues supersonic CO_2 nanobullets into the air at atmospheric pressure. The developed process uses the CO_2 gas that is captured from other industrial sites, and thus it is environmentally benign and free of harmful environmental wastes. Furthermore, the CO_2 cleaning at atmospheric conditions can save the cost and energy consumption needed to create vacuum. We adopted a single-phase compressible flow theory to compute key design parameters, such as the area ratio of exit and throat and the gas supply pressure, and examined the results with a model considering the phase change. It was shown that our nozzle is capable of generating CO_2 nanobullets into the atmospheric back pressure while the conventional nozzles used for vacuum back pressure fail to produce stable CO_2 aerosols. We also investigated the effects of the stand-off distance and incident angle of the CO_2 beam on the particle removal efficiency, to provide a set of optimal process conditions.

The design methodology delineated in this work allows us to design nozzles that produce supersonic nanobullets from various kinds of gas, including nitrogen, and argon as well as CO_2, into the air at atmospheric pressure. Even with the high-momentum nanobullets, the cleaning efficiency and pattern-damaging probability varies with the stand-off distance and incident angle, requiring us to optimize those fluid-dynamic conditions. The maximum speed of the particle beam is limited under the atmospheric pressure condition. In addition, the nanobullets may exchange heat with the surrounding air and sublimate back to the gas. Therefore, the process parameters should be carefully chosen to operate in the atmospheric condition. Since our nozzle designed for the atmospheric back pressure has been shown to work equally well for lower back pressure, our nozzle can expand the process windows in the semiconductor cleaning. The proposed cleaning system employing no additional facilities like chillers, vacuum chambers and carrier gas handling apparatus provides huge advantages over conventional wet cleaning and vacuum-chamber-based CO_2 cleaning schemes.

Acknowledgements This work was supported by National Research Foundation of Korea (Grant No. 2018052541) and SEMES Co., Ltd. via SNU IAMD.

Compliance with ethical standards

Conflict of interest Patent concerning the CO_2 cleaning at atmospheric condition is pending (USA patent # 15/769, 367, 2018, China patent # 201680063511.5, 2018, Korea patent # PCT/KR2016/011816, 2016).

References

1. Busnaina, A. A., Lin, H., Moumen, N., Feng, J. W., & Taylor, J. (2002). Particle adhesion and removal mechanisms in post-CMP cleaning processes. *IEEE Transactions on Semiconductor Manufacturing*, *15*, 374.
2. Association, S. I. (2003). *International Technology Roadmap for Semiconductors*
3. Menon, V. B. (1990). *Particle control for semiconductor manufacturing*. New York: Marcel Dekker.
4. Kern, W. (Ed.). (1993). *Handbook of semiconductor wafer cleaning technology*. Park Ridge: Noyes.
5. Rimai, D. S., & Quesnel, D. J. (2001). *Fundamentals of particle adhesion*. Moorhead: Global Press.
6. Takahashi, M., Liu, Y. L., Narita, H., & Kobayashi, H. (2008). Si cleaning method without surface morphology change by cyanide solutions. *Applied Surface Science*, *254*, 3715.
7. Kim, W., Kim, T. H., Choi, J., & Kim, H. Y. (2009). Mechanism of particle removal by megasonic waves. *Applied Physics Letters*, *94*, 081908.
8. Reinhardt, K. A. (2011). *Handbook of cleaning for semiconductor manufacturing*. Hoboken: Wiley.
9. Kern, W. (1990). The evolution of silicon wafer cleaning technology. *Journal of the Electrochemical Society*, *137*, 1887.
10. Mastrangelo, C. H., & Hsu, C. H. (1993). Mechanical stability and adhesion of microstructures under capillary forces-part I: Basic theory. *Journal of Microelectromechanical Systems*, *2*, 33.
11. Mastrangelo, C. H., & Hsu, C. H. (1993). Mechanical stability and adhesion of microstructures under capillary forces-part II: Experiments. *Journal of Microelectromechanical Systems*, *2*, 44.
12. Kim, T. H., Kim, J., & Kim, H. Y. (2016). Evaporation-driven clustering of microscale pillars and lamellae. *Physics of Fluids*, *28*, 022003.
13. Hwang, K. S., Lee, K. H., Kim, I. H., & Lee, J. W. (2011). Removal of 10-nm contaminant particles from Si wafers using argon bullet particles. *Journal of Nanoparticle Research*, *13*, 4979.
14. Hwang, K. S., Lee, M. J., Yi, M. Y., & Lee, J. W. (2009). Removing 20 nm ceramic particles using a supersonic particle beam from a contoured laval nozzle. *Thin Solid Films*, *517*, 3866.
15. Pereira, O., Rodriguez, A., Barreiro, J., Fernandez-Abia, A. I., & de Lacalle, L. N. L. (2017). Nozzle design for combined use of MQL and cryogenic gas in machining. *International Journal of Precision Engineering and Manufacturing Green Tech*, *4*, 87.
16. Liewald, M., Tovar, G.E.M., Woerz, C., & Umlauf, G. (2019). "Tribological conditions using CO_2 as volatile lubricant in dry metal forming", Int. J. Precis. Eng. Manuf.-Green Tech. pp. 1–9
17. Kim, I., Hwang, K., & Lee, J. (2012). Removal of 10-nm contaminant particles from Si wafers using CO_2 bullet particles. *Nanoscale Research Letters*, *7*, 211.
18. Kim, M. S., Kim, T., & Park, J. G. (2015). Removal of nano-sized particles using carbon dioxide (CO_2) gas cluster cleaning without pattern damage. *Particulate Science and Technology*, *33*, 558.
19. Choi, H., Kim, H., Yoon, D., Lee, J. W., Kang, B. K., Kim, M. S., et al. (2013). Development of CO_2 gas cluster cleaning method and its characterization. *Microelectronic Engineering*, *102*, 87.
20. Sinha, S., Wyslouzil, B. E., & Wilemski, G. (2009). Modeling of H_2O / D_2O condensation in supersonic nozzles. *Aerosol Science and Technology*, *43*, 9.
21. Yang, Y., Walther, J. H., Yan, Y., & Wen, C. (2017). CFD modeling of condensation process of water vapor in supersonic flows. *Applied Thermal Engineering*, *115*, 1357.
22. Anderson, J. D, Jr. (1991). *Fundamentals of aerodynamics* (2nd ed.). New York: McGraw-Hill.

23. Xu, J., & Zhao, C. (2007). Two-dimensional numerical simulations of shock waves in micro convergent-divergent nozzles. *International Journal of Heat and Mass Transfer*, *50*, 2434.
24. Raman, S. K., & Kim, H. D. (2018). Solutions of supercritical CO_2 flow through a convergent-divergent nozzle with real gas effects. *International Journal of Heat and Mass Transfer*, *116*, 127.
25. Norman, M. L., & Winkler, K. H. A. (1985). Supersonic jets. *Los Alamos Sci.*, *12*, 38.
26. Vukalovich, M. P., & Altunin, V. V. (1968). *Thermophysical properties of carbon dioxide*. London: Collet's Ltd.
27. Fox, R. W., McDonald, A. T., & Pritchard, P. J. (2004). *Introduction to fluid mechanics* (6th ed.). Hoboken: Wiley.
28. Hill, P. G. (1966). Condensation of water vapour during supersonic expansion in nozzles. *Journal of Fluid Mechanics*, *25*, 593.
29. Saad, M. A. (1992). *Compressible fluid flow* (2nd ed.). Upper Saddle River: Prentice-Hall.
30. Toscano, C., & Ahmadi, G. (2003). Particle removal mechanisms in cryogenic surface cleaning. *Journal of Adhesion*, *79*, 175.
31. Zhang, F., Busnaina, A. A., Fury, M. A., & Wang, S. Q. (2000). The removal of deformed submicron particles from silicon wafers by spin rinse and megasonics. *Journal of Electronic Materials*, *29*, 199.
32. Banerjee, S., & Campbell, A. (2005). Principles and mechanisms of sub-micrometer particle removal by CO_2 cryogenic technique. *Journal of Adhesion Science and Technology*, *19*, 739.

Jae Hong Lee received his B.S. degree from Seoul National University in mechanical engineering. He is currently a Ph.D. candidate in the Department of Mechanical Engineering at Seoul National University. His research interests include nanoscale flows and interfacial dynamics.

Joonoh Kim received his B.S. degree from Korea University in mechanical engineering. He is currently a Ph.D. candidate in the Department of Mechanical Engineering at Seoul National University. His research interests include multiphase flows and spray dynamics.

Seungho Kim received his B.S. degree from Hongik University in mechanical & system design engineering and Ph.D. degree from Seoul National University in the Department of Mechanical Engineering. He is currently a postdoctoral associate in the Department of Biological and Environmental Engineering at Cornell University. His research interests include microfluid and biofluid mechanics.

Joongha Lee received his M.S. degree from Seoul National University in mechanical engineering. He is currently working for a company as a staff engineer. His research interests include multiphase flows and inkjet applications.

Jinkyu Kim received his Ph.D. from Saitama University in 2008. He is a senior engineer at R&D Center of SEMES. His main research interest is developing nozzle for semiconductor equipment.

Kihoon Choi received his B.S. degree from Hoseo University in mechanical engineering. He is currently a senior engineer at R&D Center of SEMES. His research interests include physical cleaning and supercritical process.

Ho-Young Kim received his B.S. degree from Seoul National University and M.S. and Ph.D. degrees from MIT all in mechanical engineering. He is now a Professor of mechanical engineering at Seoul National University. His research activities revolve around microfluid mechanics, biomimetics, and soft matter physics.